

# A wall damping method to estimate the gap resonance in side-by-side offloading problems

Yujie Liu\*, Jeffrey Falzarano

Texas A&M University, College Station, TX, USA

## ARTICLE INFO

### Keywords:

Potential theory  
Side-by-side offloading  
Gap resonance  
Artificial damping  
Wave elevation

## ABSTRACT

In the side-by-side offloading problem, the gap resonance is usually overestimated by the potential theory based methods. This article reviews the up-to-date research on this topic and discusses the existing methods to modify the potential method, in order to obtain a reasonable estimate of the wave elevation. Then a wall damping method is proposed to damp out the wave elevation. This method models the energy loss on the ship hull surface. Thus, a lid is no longer needed.

The validity of the method is established through comparisons against the experimental data. Consistent results are obtained for the wave gauge in the middle of the gap. This method is the first step to develop the categories of methods without lid. The motivation is to use the small amount of measured data and a simplified model to generate engineering acceptable results. Given more data, more improvements can be made upon this method and a more general and powerful model can be developed in the future.

## 1. Introduction

The side-by-side offloading is one type of configurations when the FLNG offloads the liquefied natural gas to the LNGC nearby. It is very challenging because the two ships stay closely to each other, forming a narrow gap between the two giant floaters. Inaccurate estimation of the interaction effects may lead to unexpected damage or collision of the ships. In the theoretical research and experimental study, it is observed that the wave resonance will happen inside the gap at some incident wave frequencies. It is unclear how much effect the wave resonance will cause to the two-body system. That is the reason why it is of growing interest to understand the phenomenon happening inside the gap and how to estimate the effects from the wave resonance on the two-body system.

This problem arises when the researchers were studying the interactions of multiple floaters using the panel method based on the potential theory. An unphysical resonance was observed inside the gap between the two large floaters. As a result, the wave elevation and the interaction force predicted by the panel method are too high based on one's physical intuitive. Thus, researchers began to investigate the phenomenon and to seek for an approach to damp out the energy which results in unreasonable wave elevation.

In the study of the 2D problem, Miao et al. (2001) investigated the problem using the linear potential theory. They identified the strong

interactions between the two floaters close-by and recommended more study for 3D cases. Saitoh et al. (2006) investigated the problem in 2D through the series of experiments. They studied the effects of gap width, draft on the wave height inside the gap.

Faltinsen et al. (2007) proposed the domain decomposition method, breaking down the problem into several domains. Meanwhile, more unknowns and more equations about the boundaries of the different domains are introduced. Singular characters of the traces are considered in formulating the local solutions of the complex velocities at edges. Finally, the analytically oriented solution is obtained to predict the piston-like sloshing in a moonpool. Kristiansen and Faltinsen (2008) tried the vortex tracking method and concluded that the vortex shedding inside the gap may lead to part of the energy loss.

Later, as the twin paper with Faltinsen et al. (2007), Faltinsen and Timokha (2015) introduced a dynamic boundary condition inside the gap and resolve the potential problem. The dynamic boundary condition is based on the pressure drop estimation and empirical formulas on some coefficients. By modeling the dynamic free surface, it becomes unnecessary to model the complex phenomenon happening inside the fluid domain. The results of such methods show a good agreement with the experimental data.

Liu et al. (2012) added a damping free surface near the floater and also decomposed the domain into several parts with damped boundary condition on the vertical surfaces. Damping happens on the gap free

\* Corresponding author. Marine Dynamics Laboratory, Department of Ocean Engineering, Texas A&M University, College Station, TX, 77843-3136, USA.  
E-mail address: [yjliu2012@tamu.edu](mailto:yjliu2012@tamu.edu) (Y. Liu).

surface and the interface of the boundaries. By matching the experimental data, the author proposed a linear model to fit the damping coefficient against characteristics of the box and fluid domain.

In the study of 3D problems, Buchner et al. (2004) proposed the lid method inside the gap. They enforced the no-penetration condition on the lid and found this method can suppress the resonance. Later, Chen (2005) proposed the damping lid method. They added a dissipative term in the free surface boundary condition inside the gap. Chen and Malenica (2005) discussed the damping method applied in the multi-body problem. The authors introduced damping coefficients for the free surface boundary condition and the body boundary conditions. The method basically reduced the source strength by adjusting the terms associated with the damping effects. However, one needs to tune the damping coefficients on the free surface and body boundary by comparison against the experimental data. Meanwhile, by modifying the equations of the system, it is likely that the resonance frequency will have a tiny shift with a nonzero damping coefficient. This method was used by Pauw et al. (2007), Bunnik et al. (2009) and Lu et al. (2011). They all reported satisfactory results can be obtained by this method.

Zhu et al. (2005) treated the 3D side-by-side problem by the linear potential method in frequency domain, investigated the effect of the gap width on the resonant frequency and amplitude. Teigen and Niedzwecki (2006) applied the panel method up to second order to investigate the problem. They concluded that the wave amplification inside the gap is sensitive to the wave frequency and wave heading. The surprising second order effect is observed around the two barges. Zhu et al. (2006) studied the effect of gap in the multiple boxbarge problems. Only the radiation potential was considered herein. They concluded that the sway motion showed a strong interaction effect at certain wave number. Sun et al. (2010) applied 1st and 2nd order panel method to investigate the dependency of the wave elevation on box motion, spacing, wave direction, draft. They observed a similar behavior in 1st order and 2nd order potential along the gap. Markeng (2017) investigated pressure damping method and Newtonian cooling damping model in 2D cases and implemented the latter one in the 3D potential flow solver. The authors concluded the Newtonian cooling damping model is relatively more effective to model the resonance. The damping coefficient still needs to be tuned against the experimental data.

Zhao et al. (2016) conducted the experiment to study two identical box barges side-by-side. The two boxbarges are fixed. In the experiments, different modes of gap resonance have been observed. This is a very good resource to study the side-by-side problems because the experiment has eliminated the effects of the ship motion and focuses on the diffraction effects. It will be helpful to understand the physical mechanism. Zhao et al. (2017b) discussed about the damping effects and mentioned that for the round bilge cases, the viscous effects from the hull surface seem to be more significant than the flow separation effects. Zhao et al. (2017a) pointed out that the viscosity mainly leads to the discrepancy between linear potential theory and the experimental data. The authors compared the results from different commercial software and benchmarked against the experimental data.

In this paper, we categorize the existing artificial damping methods into two types: the domain decomposition method and the lid method. We review the two types of methods first. Inspired by the researchers, we propose the wall damping method to model the energy loss on the ship hull surface, in order to obtain a reasonable prediction of wave elevation inside the gap. Finally, the results are benchmarked against the experimental data. The achieved consistency shows that our method is effective. The proposed wall damping method considers the physical effects, which is the significant difference from the lid method applied directly on the free surface inside the gap. It can evolve into a more advanced and robust method given more experimental data.

## 2. Review of artificial damping methods

In this section, we discuss the previous works on artificial damping methods and also describe our proposed method. Before proceeding to the derivation, we review the formulas for the 1st order seakeeping problem, which is the basis of the damping methods.

The nonlinear kinematic and dynamic boundary conditions of the hydrodynamic problem are:

$$\frac{\partial \zeta}{\partial t} + \frac{\partial \Phi}{\partial x} \frac{\partial \zeta}{\partial x} + \frac{\partial \Phi}{\partial y} \frac{\partial \zeta}{\partial y} = \frac{\partial \Phi}{\partial z} \quad \text{at } z = \zeta(x, y, t) \quad (1)$$

$$\frac{\partial \Phi}{\partial t} + \frac{1}{2} \nabla \Phi \cdot \nabla \Phi + g\zeta = C - \frac{p_a}{\rho} \quad \text{at } z = \zeta(x, y, t) \quad (2)$$

After applying the perturbation technique and Taylor expansion, we obtain the 1st order equation as below:

$$\frac{\partial \zeta^{(1)}}{\partial t} = \frac{\partial \Phi^{(1)}}{\partial z} \quad \text{at } z = 0 \quad (3)$$

$$\frac{\partial \Phi^{(1)}}{\partial t} + g\zeta^{(1)} = 0 \quad \text{at } z = 0 \quad (4)$$

In solving for the Green function, we usually merge the two equations to get the combined free surface boundary condition:

$$\frac{1}{g} \frac{\partial^2 \Phi^{(1)}}{\partial t^2} + \frac{\partial \Phi^{(1)}}{\partial z} = 0 \quad \text{at } z = 0 \quad (5)$$

With the Green function, we solve for the source strength using the body boundary condition.

$$\vec{n} \cdot \nabla \Phi^{(1)} = \vec{n} \cdot \vec{V}^{(1)} \quad \text{at body surface} \quad (6)$$

By assuming steady state, we can apply the following equations and make the equations independent of time  $t$ .

$$\Phi^{(1)} = \text{Re} \{ \phi^{(1)} e^{i\omega t} \}$$

$$V_n = \text{Re} \{ v_n e^{i\omega t} \}$$

$$\zeta^{(1)} = \text{Re} \{ \zeta^{A(1)} e^{i\omega t} \}$$

Then the body boundary condition becomes:

$$\frac{\partial \phi^{(1)}}{\partial n_x} = -\frac{1}{2} \sigma(x) + \frac{1}{4\pi} \iint_{S_b} \sigma(\xi) \frac{\partial G(x; \xi)}{\partial n_x} dS_\xi = v_n \quad (7)$$

Afterwards, substituting the source strength on the body into the following equation, we obtain the potential at any point inside or on the boundary of the fluid domain:

$$4\pi \phi^{(1)}(x) = \iint_{S_b} \sigma(\xi) G(x; \xi) dS_\xi, \quad x \in S_b \cup V \quad (8)$$

Using equation (4), we will be able to find the wave elevation on the linearized free surface. The equation for the complex amplitude is as below:

$$\zeta^{A(1)} = -\frac{i\omega \phi^{(1)}}{g} \quad (9)$$

The nondimensional form is:

$$\bar{\zeta}^{A(1)} = \frac{\zeta^{A(1)}}{A} = -\frac{i\omega \phi^{(1)}}{Ag} \quad (10)$$

where,  $A$  is the wave amplitude.

When we observe a very high wave elevation, the potential value at the point of interest is naturally large. To reduce the wave elevation, it is straightforward to put a rigid lid on the gap as discussed in Buchner et al. (2001). A rigid lid may be too strong a restriction on the gap free surface. Later, the damping lid method was proposed in Chen (2005). The wave elevation along the gap is reduced especially at resonant frequencies. When we add damping terms on the gap free surface, we are changing the source strength on the body panels and then the

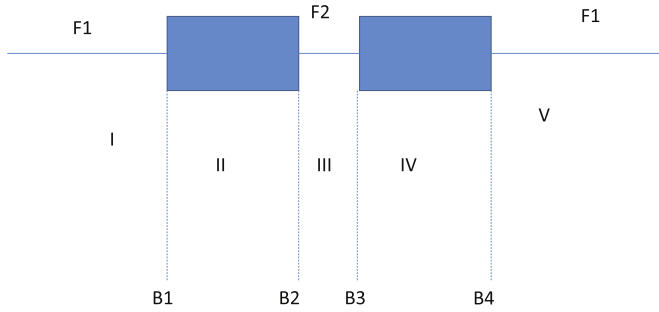


Fig. 1. Example Configuration for domain decomposition method.

potentials throughout the domain. If we can decompose the domain into several parts and control the interfaces of the subdomains. We may also achieve a reduced wave elevation. Different types of the domain decomposition methods were discussed in [Faltinsen et al. \(2007\)](#), [Liu et al. \(2012\)](#), etc. In the following two sections, we discuss the mathematical concepts of the lid method and the domain decomposition method.

### 2.1. The domain decomposition method

The domain decomposition method breaks down the original solution domain (fluid domain herein) into several parts. It leads to a system of integral equations on the interfaces of the domains, also known as the transmission interfaces. The concept can be illustrated in [Fig. 1](#).

[Fig. 1](#) is to illustrate the idea of the method. It may have some differences from the discussions in different papers.  $F1, F2, F3$  stand for the free surfaces around the floaters.  $I, II, III, IV, V$  are the subdomains.  $B1, B2, B3, B4$  are the interfaces between the subdomains. Proper transmission conditions need to be specified on the interfaces  $B1, B2, B3, B4$ . In [Faltinsen et al. \(2007\)](#), the authors introduced admissible functions on the interfaces. Then they solved the problem in different domains separately. In [Liu et al. \(2012\)](#), a dissipation boundary condition is introduced in the gap free surface  $F2$  and also on  $B1, B4$ . The boundary condition restricted the transmission of energy from domain to domain, in order to ensure a reasonable wave elevation inside the gap. The change in the solution system can be illustrated as in [Fig. 2](#).

This method is mainly applied in the 2D problem. If considering the 3D case, one may need to decide where to place the interfaces of the domains and also tune the unknown damping coefficients on the transmission boundary conditions to make the simulated wave elevation consistent with the experimental data.

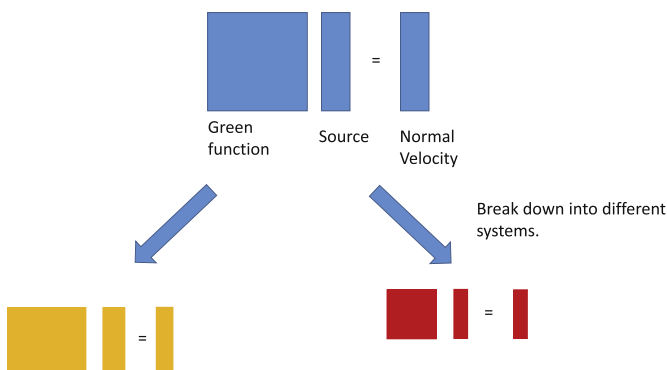


Fig. 2. Solution system for domain decomposition method.

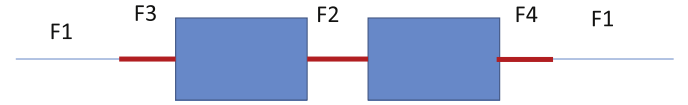


Fig. 3. Example Configuration for damping lid method.

### 2.2. The lid method

The lid method is also an effective method to damp out the wave elevation of the gap free surface. It can be applied in 2D and 3D problem. The methods are already included in some commercial software, for example, WADAM and HydroSTAR.

This method modifies the boundary condition on part of the free surface. To consider the change in the equation system, the part of the free surface needs to be panelized and the source strength on the panels need to be solved. That may be the reason why it is called "lid method". The concept can be shown in [Fig. 3](#).

In [Fig. 3](#),  $F1$  stands for the part of the free surface without damping.  $F2, F3, F4$  are the parts, on which the damping terms may be included. Typically, only  $F2$  is panelized. Sometimes,  $F3, F4$  or some places inside the fluid domain is also panelized to incorporate the damping effect.

The mathematical essence of this method is to introduce more unknowns, constructing a bigger matrix. It is similar to the irregular frequency removal method discussed in [Liu and Falzarano \(2016a\)](#) and [Liu and Falzarano \(2017a\)](#). The concept can be shown in [Fig. 4](#).

#### 2.2.1. The Newtonian damping method

There are two similar techniques belonging to this category. One is the Newtonian cooling method. This method was discussed in [Kim \(2003\)](#), [Markeng \(2017\)](#). The damping effect is enforced on the first order kinematic free surface condition. We have the modified kinematic free surface boundary condition:

$$\frac{\partial \zeta^{(1)}}{\partial t} = \frac{\partial \Phi^{(1)}}{\partial z} \quad \text{at } z = 0 \quad (11)$$

$$\frac{\partial \Phi^{(1)}}{\partial t} + g \zeta^{(1)} = 0 \quad \text{at } z = 0 \quad (12)$$

$$\frac{\partial \zeta^{(1)}}{\partial t} = \frac{\partial \Phi^{(1)}}{\partial z} - a \zeta^{(1)} + \frac{b}{g} \Phi^{(1)} \quad \text{at } z = 0 \quad (13)$$

where,  $a, b$  are the coefficients to denote the linear relationship. According to [Markeng \(2017\)](#), we can select  $a, b$  so that the dispersion relationship remains the same. Herein we will explore the process to decide on the value or the relationship between  $a, b$ , the coefficients in

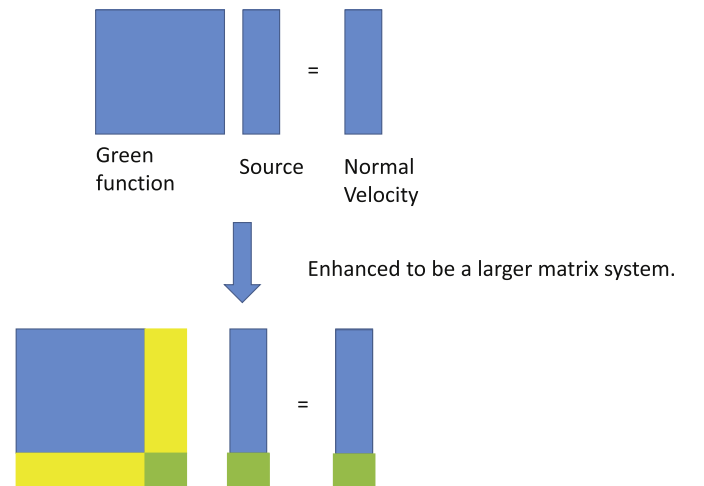


Fig. 4. Solution system for damping lid method.

equation (13).

If using the original dynamic boundary condition and the modified kinematic free surface boundary condition 13, we get the modified combined free surface boundary condition:

$$\frac{\partial^2 \Phi^{(1)}}{\partial t^2} + g \frac{\partial \Phi^{(1)}}{\partial z} + a \frac{\partial \Phi^{(1)}}{\partial t} + b \Phi^{(1)} = 0 \quad (14)$$

In deriving the dispersion relationship, we assume  $\Phi^{(1)}$  satisfies  $\Phi^{(1)}(x, z, t) = X(x)Z(z)T(t)$ . Substituting the equation into the combined free surface boundary condition, we have:

$$T'' + g \frac{Z'}{Z} T + a T' + b T = 0 \quad (15)$$

From wave potential for the deep water condition, we know  $Z$  satisfies  $Z' = kZ$ , where  $k$  is the wave number. The above equation becomes:

$$T'' + gkT + aT' + bT = 0 \quad (16)$$

Mathematically, we need to solve for this equation to find the solution for  $T$ . Here we are reverse engineering the previous references. Thus, we may introduce some assumptions to explore the relationship. If  $T$  satisfies  $T' = i\omega T$ ,  $T'' = -\omega^2 T$ , we obtain the equation about the wave frequency  $\omega$ :

$$-\omega^2 + gk + i\omega a + b = 0 \quad (17)$$

Then we have:

$$\begin{aligned} \omega^2 - i\omega a - \frac{a^2}{4} &= gk + b - \frac{a^2}{4} \\ \omega &= \pm \sqrt{gk + b - \frac{a^2}{4}} + i\frac{a}{2} \end{aligned} \quad (18)$$

If  $b = a^2/4$ ,  $\omega = \sqrt{gk} + ia/2$ , where the real part of  $\omega$  is  $\sqrt{gk}$ . If we take  $a = 2\mu$ ,  $b = \mu^2$ , we get the exactly same equations as in Markeng (2017) as below:

$$\frac{\partial \zeta^{(1)}}{\partial t} = \frac{\partial \Phi^{(1)}}{\partial z} - 2\mu \zeta^{(1)} + \frac{\mu^2}{g} \Phi^{(1)} \quad \text{at } z = 0 \quad (19)$$

When calculating the wave elevation, the dynamic free surface boundary condition may be applied to calculate the wave elevation.

$$\zeta^{(1)} = -\frac{1}{g} \frac{\partial \Phi^{(1)}}{\partial t} = -\frac{i\omega}{g} \Phi^{(1)} \quad (20)$$

If we take the  $\omega = \sqrt{gk} + ia/2$ , the wave elevation becomes:

$$\zeta^{(1)} = -\frac{i\sqrt{gk}}{g} \Phi^{(1)} + \frac{\mu}{g} \Phi^{(1)} \quad (21)$$

When tuning the value of  $\mu$  against the experimental data, we are almost directly changing value of wave elevation.

Additionally, the combined free surface boundary condition becomes:

$$\frac{\partial \Phi^{(1)}}{\partial z} = \frac{1}{g} [\omega^2 - 2i\omega\mu - \mu^2] \Phi^{(1)} = \frac{(\omega - i\mu)^2}{g} \Phi^{(1)} \quad (22)$$

To consider the change of the free surface boundary condition, the gap surface needs to be panelized. The above formula will be applied in the surface integral to solve for the source strength.

To conclude, the Newtonian damping method provides an approach to adjust the wave elevation inside the gap. A different free surface boundary condition is applied inside the gap. If applying the same Green function, a lid is needed along the gap free surface. The introduction of the damping terms will affect both the equation system to solve for the potential value or the source strength and the calculation of the wave elevation. To decide on a reasonable damping coefficient, one needs to tune it against the experimental data. This is a mathematical way to modify the method based on potential theory. The process to derive the revised dispersion relationship may not be strictly

accurate. Additionally, if the wave frequency has an imaginary part and we continue using the formula  $\Phi^{(1)} = \text{Re}\{\phi^{(1)}e^{i\omega t}\}$ , the term  $\phi^{(1)}$  may not be independent of time.

### 2.2.2. XB Chen's damping method

Another very promising approach is the method proposed by Chen and Malenica (2005). The damping force is applied in the dynamic free surface boundary condition. The amplitude of the force is proportional to the amplitude of the velocity on the free surface.

The formula is as below:

$$\vec{F} = -\mu \vec{V} \quad (23)$$

In the dynamic free surface boundary condition, if we apply the damping force, the equation becomes:

$$\left(\frac{\partial}{\partial t} + \vec{V} \cdot \vec{\nabla}\right) \vec{V} = -\vec{\nabla} \left(\frac{P}{\rho} + gz\right) - \mu \vec{V} \quad \text{on } z = \zeta(x, y, t) \quad (24)$$

If assuming ideal flow, the velocity can be expressed in terms of the potential as  $\vec{V} = \vec{\nabla} \Phi$ . Then the equation is:

$$\left(\frac{\partial}{\partial t} + \vec{\nabla} \Phi \cdot \vec{\nabla}\right) \vec{\nabla} \Phi = -\vec{\nabla} \left(\frac{P}{\rho} + gz\right) - \mu \vec{\nabla} \Phi \quad (25)$$

$$\frac{\partial \Phi}{\partial t} + \frac{1}{2} \vec{\nabla} \Phi \cdot \vec{\nabla} \Phi + \frac{P}{\rho} + gz + \mu \Phi = C(t) \quad \text{on } z = \zeta(x, y, t) \quad (26)$$

Making the same choice for pressure  $P$  and the constant  $C(t)$ , we can extract the first order  $o(\epsilon)$  part of the dynamic free surface boundary condition:

$$\frac{\partial \Phi^{(1)}}{\partial t} + g \zeta^{(1)} + \mu \Phi^{(1)} = 0 \quad \text{on } z = 0 \quad (27)$$

The wave elevation becomes:

$$\begin{aligned} \zeta^{(1)} &= -\frac{1}{g} \left( \mu \Phi^{(1)} + \frac{\partial \Phi^{(1)}}{\partial t} \right) \\ &= -\frac{\mu + i\omega}{g} \Phi^{(1)} \\ &= -\frac{i\omega}{g} \Phi^{(1)} - \frac{\mu}{g} \Phi^{(1)} \end{aligned} \quad (28)$$

If substituting the wave elevation into the kinematic free surface boundary condition, we obtain a combined formula:

$$-\frac{1}{g} \frac{\partial}{\partial t} \left( \mu \Phi^{(1)} + \frac{\partial \Phi^{(1)}}{\partial t} \right) = \frac{\partial \Phi^{(1)}}{\partial z} \quad (29)$$

Rearranging the terms, we obtain:

$$\begin{aligned} \frac{\partial \Phi^{(1)}}{\partial z} &= \frac{\omega^2}{g} \left( 1 - i\frac{\mu}{\omega} \right) \Phi^{(1)} \\ &= \frac{\omega^2}{g} \Phi^{(1)} - i\frac{\omega\mu}{g} \Phi^{(1)} \end{aligned} \quad (30)$$

Applying the similar technique, we can get the relationship that  $\omega$  and  $k$  satisfy:

$$\omega^2 - gk - i\omega\mu = 0 \quad (31)$$

Solving for  $\omega$ , we get:

$$\omega = \pm \sqrt{gk - \frac{\mu^2}{4}} + \frac{i\mu}{2} \quad (32)$$

The real part of the wave frequency is no longer  $\sqrt{gk}$  and  $\omega$  contains an imaginary part as well.

In this method, the free surface boundary condition inside the gap is also changed. Thus, the gap surface needs to be panelized. The damping coefficient has changed the matrix to solve for the potential value or the source strength. It also appears in formula (28) to calculate the wave elevation. Intuitively speaking, when we want to consider the damping effect, we deduct a portion from the original wave elevation. However,

if we consider the term related to damping effect, we have also changed the value of the potential. It is indicating that we probably need to tune the damping coefficient for several rounds to make the simulation results match the experimental data.

This method is an alternative approach to modify the wave elevation mathematically. It has changed the dispersion relationship inside the gap surface and the dynamic free surface boundary condition. When applying this method, one needs to decide where is the damping zone and how large it is. The choices may depend on the experience of the user.

### 3. Wall damping method

#### 3.1. Motivation

Considering the disadvantages of the above methods, two questions come: can we develop a method which does not require the user to specify where the damping zone or damping lid is? Can we use the information of the potential method without damping to identify the damping coefficients?

Let's review the physical processes first. In the potential method, the fluid is assumed to be ideal flow, which is inviscid and irrotational. The energy dissipation caused by the viscous effect is neglected in the results generated by the potential method. However, in reality, the fluid is viscous and rotational.

When comparing the results by potential method and the experimental data, we may attribute the discrepancies to the differences in the assumptions of the fluid property. Therefore, we say that it may be the viscous effects that damps out the wave elevation.

In the damping lid method, the free surface boundary condition inside the gap is directly controlled to ensure a reasonable wave elevation. It is a straight forward approach to adjust the wave elevation. In this way, the distribution of the potential value will be affected by the change in the free surface boundary condition.

In the domain decomposition method, the fluid domain is broken down into several parts. The transmission of the energy is controlled on the interfaces of the subdomains and the damping condition is also enforced on the free surface inside the gap. As a result, the wave elevation is ensured to be reasonable and the potential throughout the domain is likely to be altered.

The two types of approaches provide feasible ways to modify the matrix structure to solve for the source strength of the potential value on the ship hull. Through the modifications, a reasonable wave elevation can be obtained.

In the potential method without damping, the body boundary condition will determine the source strength or the potential value on the ship hull. In [Chen and Malenica \(2005\)](#), the authors discuss the damping condition on the ship hull near the gap. The damping condition was also adopted in coastal engineering to model the partial reflection of a wall. In the sloshing problem, a uniform damping effect is applied on the tank surface to adjust the motion RAO of the floater as discussed in [Zalar et al. \(2007\)](#). The partial reflection is an alternative way to incorporate the damping effect of the system.

Inspired by the discussion of the partial reflection in [Chen and Malenica \(2005\)](#), we introduce damping effects of different intensities on the ship hull surface. The intensity is determined by the activity level of the fluid nearby.

Enlightened by the domain decomposition method and based on the observation of the contour plots through the potential method, we break the ship hull surface into three parts: the side shell next to the gap, the hull bottom and the side shell away from the gap. It can be shown in [Fig. 5](#).

In [Fig. 5](#), the green part stands for the side shell next to the gap. The yellow part is the side shell far away from the gap. The red part indicates the rest part of the ship. In 2D, the red part only includes the hull bottom. In 3D cases, it also includes the stern and bow in the

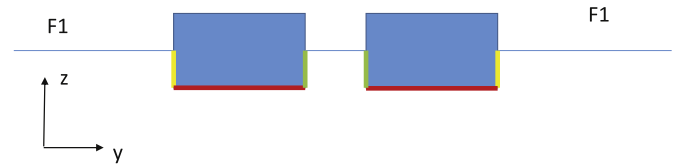


Fig. 5. Concept of the proposed method.

middle region.

To conclude, the wall damping method directly introduces the damping effect on the ship hull instead of on the free surface inside the gap. This is more physical because the energy loss may mainly happen on the ship hull rather than the free surface inside the gap, as discussed in the introduction part. To distinguish the damping effects on different sections of the ship hull, we assume different damping coefficient on different parts of the ship hull, which is inspired by the domain decomposition method. However, instead of decomposing the fluid domain, we split the ship hull into different parts.

#### 3.2. Wall damping method

##### 3.2.1. Formula

We incorporate the damping term into the body boundary condition by using this formula, following [Chen and Malenica \(2005\)](#):

$$\frac{\partial \phi^{(1)}}{\partial n_x} = v_n - i\mu \frac{\omega^2}{g} \phi \quad \text{at body surface} \quad (33)$$

If we include the damping term in the body boundary condition, the formula changes into:

$$\frac{\partial \phi^{(1)}}{\partial n_x} = -\frac{1}{2}\sigma(\mathbf{x}) + \frac{1}{4\pi} \iint_{S_b} \sigma(\xi) \left[ \frac{\partial G(\mathbf{x}; \xi)}{\partial n_x} + i\mu \frac{\omega^2}{g} G(\mathbf{x}; \xi) \right] dS_\xi = v_n \quad (34)$$

The damping term is introduced to model the partial reflection of the wall boundaries. It essentially affects the value of the source strength, which is used to calculate the potential value and the wave elevation inside the gap. If the wave elevation without damping is too high, we hope to damp out the wave elevation by tuning the damping term introduced here.

In our case, we assume the damping coefficient  $\mu$  is a function of location  $y$  and the incident wave frequency  $\omega$ :  $\mu = \mu(y, \omega)$ .  $y$  is adopted to decompose the ship hull into 3 parts and  $\mu$  will stay constant on each of the three parts of the ship hull given the frequency. We decide which region a panel falls into based on the location of its centroid. The values of  $\mu$  on different regions can be different.

##### 3.2.2. Determination of ratios

Therefore, to consider the different damping effects on the three sections of the ships, we assume the damping coefficients satisfy a ratio of  $a:b:c$ . To decide the damping coefficients in the equation, we multiply a constant  $\mu$  to the ratio. Then the damping coefficients are  $a\mu$ ,  $b\mu$ ,  $c\mu$ . Consequently, we need to decide the value of  $\mu$  and the ratio of the damping coefficients  $a:b:c$ .

In this method, we assume that the panels belonging to one section share the same damping coefficient. It is similar to adding an average damping to the section. If we assume the damping effect is positively correlated to the prediction through the potential method, we may use the ratio of the potential values to help decide the ratio of the damping coefficients.

In generating the results for wave frequencies ranging from 6.01 ~ 9.91 rad/s, we can obtain the potential value for each panel at each frequency. Herein, we assume the average effect can be achieved by two types of ratios. One ratio is obtained in this way: first summing up the potential value at each section for all frequencies, then find the mean value of the potential for each section and finally calculate the



ratio. We may name it as "ratio of the mean".

The other ratio can be named as "ratio of the max mean". Firstly, we compute the mean of the potential values for each section at a certain frequency. Then we find the ratio for each frequency. If we denote the ratio as the format "1:x:y" and  $y > x > 1$ , we can eventually find the ratio with the largest value of  $y$ . That ratio is our final selection. Please note that we will always divide each number in a ratio by the smallest number so that the ratio has 1 as the minimum value. This is a rule of notation to describe the possible relationship between the damping effects on different sections.

Herein, we provide two possible types of ratios for reference. The ratios reflect the difference in the average potential value. In practice, other types of ratios can be defined as well. The values in the ratios will affect the amplitudes of the kernel functions discussed below. The bigger number inside a ratio will lead to a smaller amplitude of the kernel function.

### 3.2.3. Kernel function

The ratios of the potential values on the 3 sections indicate the average activity level of the fluid close to the different sections. However, based on the observations, the activity level is frequency dependent. In other words, at some frequencies, especially the resonant frequencies, the amplitude of the wave elevation or the velocity of fluid inside the gap is relatively larger.

We may assume when the fluid has a relatively larger velocity, the friction effect can cause more energy loss to the system. In other words, the damping effect is positively correlated with the activity of the system. Generally, the damping effect becomes significant when reaching the resonant frequencies and it may also grow with the increasing wave radian frequency. Because the velocity amplitude of the fluid particles is growing as the frequency increases.

To consider the resonance effects, we propose to apply the Gaussian kernel function in the function of the damping coefficient  $\mu$ . The formula of  $\mu$  is expressed as:

$$\mu = \sum_i^{res} A_i \exp[-k(\omega - \omega_i^{res})] \quad (35)$$

where, "res" stands for "resonance". The number of the terms is equal to the number of resonant frequencies observed.  $A_i$  is the amplitude of the kernel functions.  $k$  is the decay ratio and  $\omega_i^{res}$  is the resonant frequencies.

In this equation,  $\omega_i^{res}$  is determined from the results of the MDLMultiDYN without the non-potential flow damping effect. The unknowns are all the  $A_i$  and the decaying factor  $k$ . Additionally, the in-house program MDLMultiDYN is developed by Liu and Falzarano (2016b) to study the hydrodynamic problems of multiple floaters. It has the module to remove irregular frequency effects (Liu and Falzarano (2017e)), has two options to evaluate the mean drift forces in (Liu and Falzarano (2017d) Liu and Falzarano (2018)) and is able to perform analysis for low-speed cases (Liu and Falzarano (2017c) Liu and Falzarano (2017b)). The program MDLMultiDYN can be used for generating the input of the evaluation of wave energy converter discussed in Wang et al. (2017) Wang et al. (2017) Wang and Falzarano (2013). MDLMultiDYN is currently for the study of the cases in deep water only. The module of finite depth Green function is under development by Xie et al. (2017) and will be incorporated into the main program, which can be applied to numerically simulate the offshore applications in frequency domain, for example, the problem discussed in Xie et al. (2015). The module of quadratic transfer function is completed by Xie et al. (2019).

Given the experimental data, we may adjust the value of  $A_i$  and  $k$  to make sure the results from the wall damping methods are consistent. We can first tune the amplitude of the kernel function for the result of each resonant frequency separately. More specifically, we tried different values of  $A_i$  at a certain frequency. Then we chose the  $A_i$  which

makes the wave elevation from simulation close to the experimental data and repeat the steps for other resonant frequencies. In this way, we can find proper values of  $A_i$ . Afterwards, by adjusting the value of  $k$ , we make the results at other frequencies approximately consistent. More specifically, we tried different values of  $k$  after we decided the values of  $A_i$  until the results are close to the experimental data. The value of  $k$  decides how fast the damping coefficient will decay from a certain resonant frequency. If the  $k$  is zero, the damping coefficient will be a constant for all frequencies. If the  $k$  is very small, it decays slowly when the frequency of interest is away from the resonant frequencies. When  $k$  is large, it decays relatively fast when the frequency of interest is shifted away from a certain resonant frequency. When  $k$  is approaching infinity, the damping coefficient will be approximately zero at all frequencies except for the resonant frequencies. If enforcing too much damping effect, the wave elevation will be relatively smaller. The objective of the tuning process is to find a proper value of  $k$  which introduces a proper amount of damping at all frequencies. In the next section, we will demonstrate the effectiveness of the wall damping method.

### 3.2.4. Discussion on wall damping method

Up till this step, we have finished the discussion of the motivation of the wall damping method, the formula and the tuning process. We discuss the advantages and possible limitations of the method in this section.

The wall damping method directly models the energy loss on the ship hull, which is more physical compared against the lid method applied on the free surface inside the gap. It does not change the dispersion relationship when enforcing the damping effects. More importantly, this method may prove that we are able to dig out more information on the damping effects based on the results from the linear potential method without damping. The model discussed here is one possible guess of the relationship between the output of the potential theory method and the experimental data. If obtaining more experimental data, we will find a better model which may be better generalized.

However, this proposed method has more free parameters to be determined than the damping lid method. The user may spend more efforts in tuning the parameters. By assuming the linear relationship of the amplitudes at the resonant frequencies, we can decrease the number of free parameters to mitigate the drawback. More details will be provided in the next section.

## 4. Results

Herein, we will mainly study the wave elevation at the wave gauge 4, which is located at the center of the gap. We apply the methods to the cases in both head sea and beam sea conditions to prove the effectiveness. Herein, we choose the "ratio of the max mean" as an example. It is equivalent to choose the other ratio, the steps remain the same. The difference may lie in the expressions of the kernel functions. To evaluate the methods, we developed the program in MATLAB, using the output of intermediate steps from MDLMultiDYN. In the comparison, the results from the MATLAB code is always on top of those from the MultiDYN when there is no damping effect, which is to validate the correctness of the MATLAB code.

### 4.1. Head sea condition

After running the case using our in-house program MDLMultiDYN, the ratios are obtained as in the table (Table 1) below:

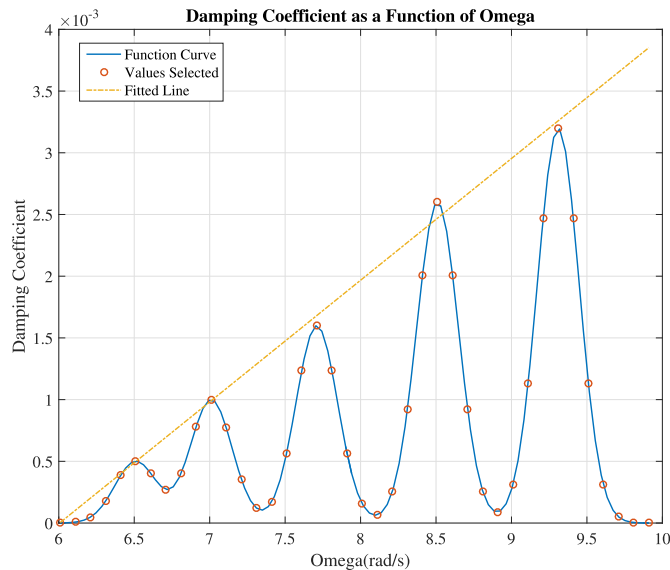
By tuning the parameters, we find the values of  $A$  are 0.0005, 0.0010, 0.0016, 0.0026, 0.0032 and the value of  $k$  is 26. The damping constant curve of  $\mu$  is shown in Fig. 6.

The circles on the curve indicate the values we selected at each frequency, which is adopted in the simulation of the MDLMultiDYN.

**Table 1**

Ratios of the potential values on the 3 sections.

Ratio	a	b	c
Ratio of the Mean	1	2.5	11
Ratio of the Max Mean	1	3	22

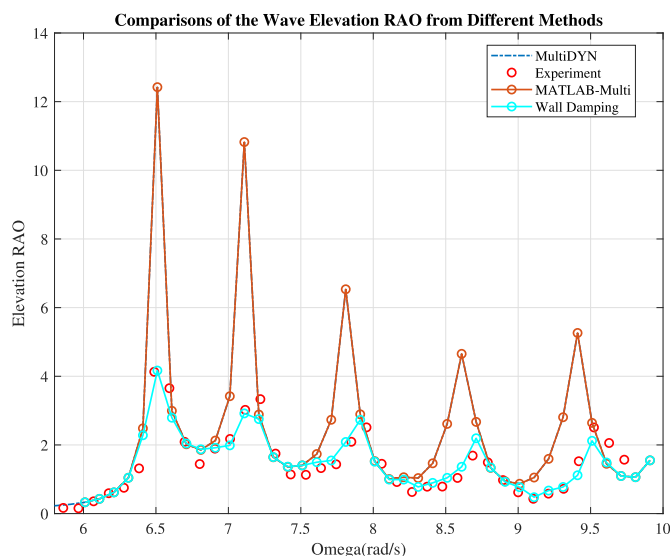
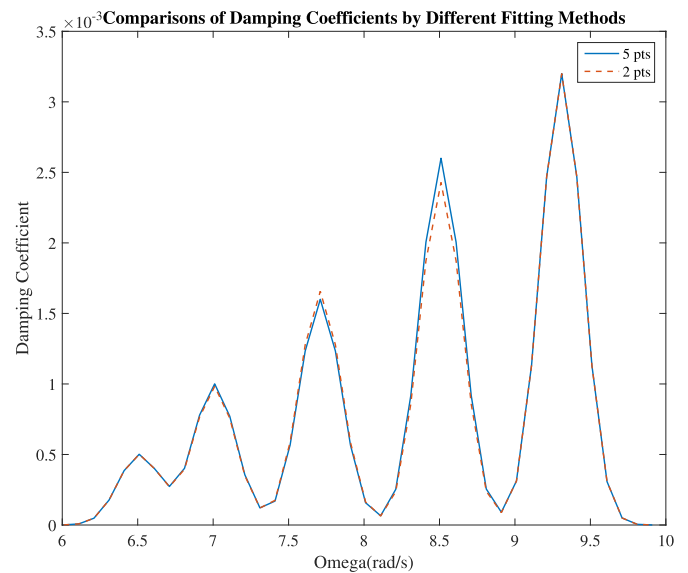
**Fig. 6.** Damping Coefficient vs Wave Frequency.

While plotting the curve, we find that the amplitudes at or near the resonant frequencies almost follow a linear relationship. On top of the curve, we also plot the fitted curve of the amplitudes. It shows that the linear curve fits well.

Applying the damping constants, we find the damping coefficient on each section at each frequency. After incorporating the damping effects, we can obtain the damped curve in Fig. 7.

From the comparisons, we can observe that the damped curve is consistent with the experimental data. The method is effective in generating a reasonable wave elevation.

In the method, we have to choose 6 parameters. Based on the linear relationship of the amplitudes at the resonant frequencies, we may just need to tune 3 parameters: the amplitudes at 2 resonant frequencies and

**Fig. 7.** Comparisons of results from modified potential method.**Fig. 8.** Comparisons of damping constants from independent tuning and linear fitting.

the parameter  $k$ . Thus, we select the amplitudes at the minimum and maximum resonant frequencies to tune and apply the fitted curve to obtain the damping constant for other amplitudes. Fig. 8 shows the difference between tuning 5 points and 2 points.

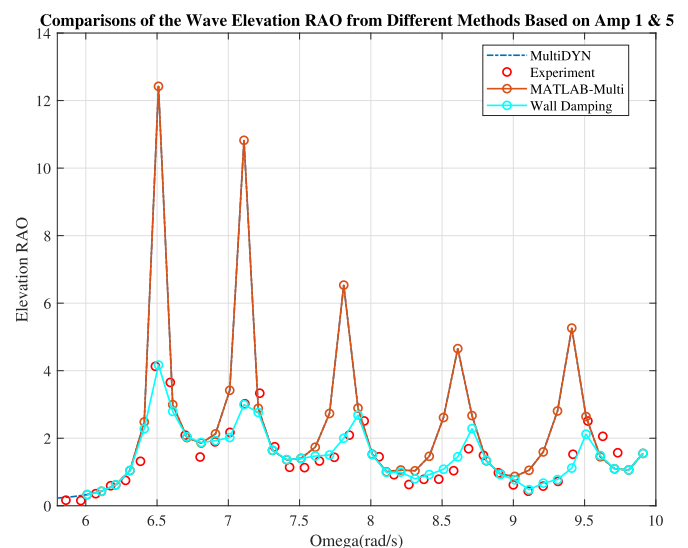
Applying the fitted curve, we obtain the curve using the modified potential method as shown in Fig. 9. It is approximately the same with that when adjusting the five amplitudes independently.

#### 4.2. Beam sea condition

Similarly, we can obtain the ratios based on the results from the potential method (Table 2).

By tuning the parameters, we find the values of  $A$  are 0.0014, 0.0020, 0.0032, 0.0042, 0.0054 and the value of  $k$  is 15. The damping constant curve of  $\mu$  is shown in Fig. 10.

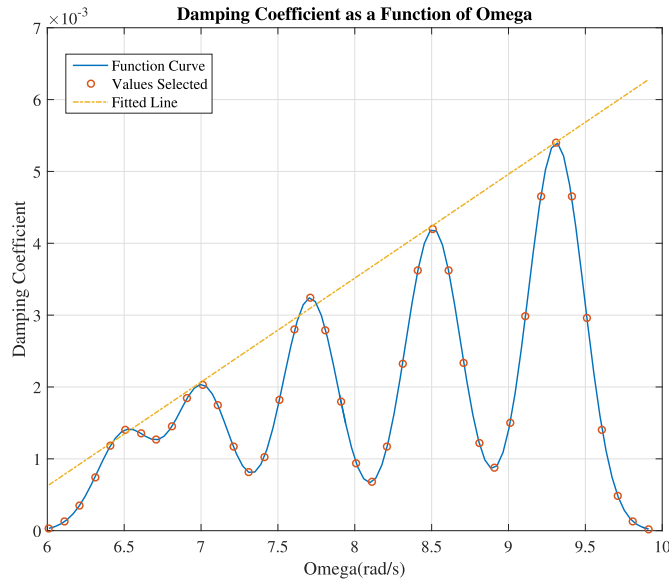
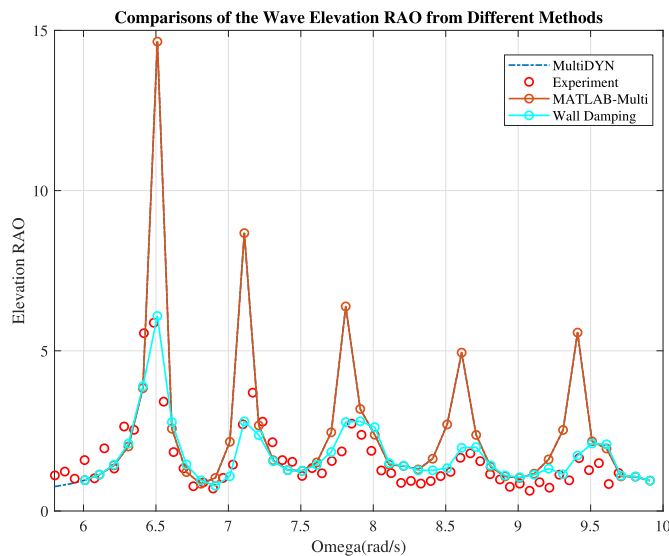
Considering the damping effects, we can obtain the results for the modified potential method as shown in Fig. 11. If we choose the 3 parameters to tune, we obtain the curves of the damping coefficients as shown in Fig. 12.

**Fig. 9.** Comparisons of results from modified potential method by tuning two amplitudes.

**Table 2**

Ratios of the potential values on the 3 sections.

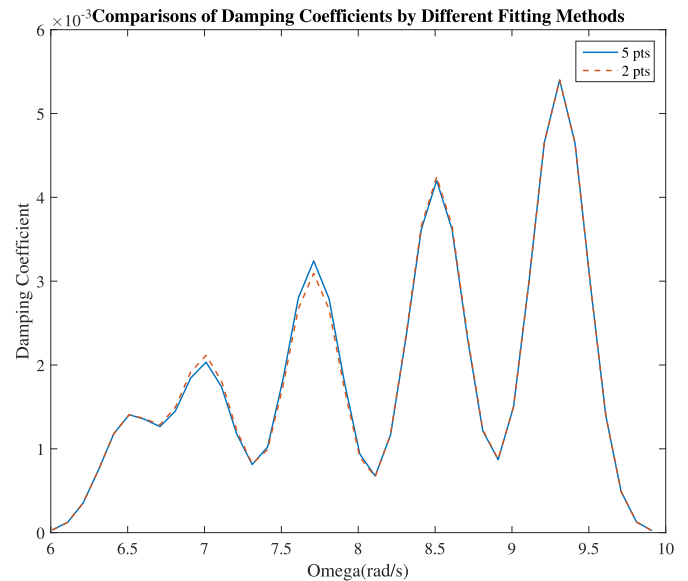
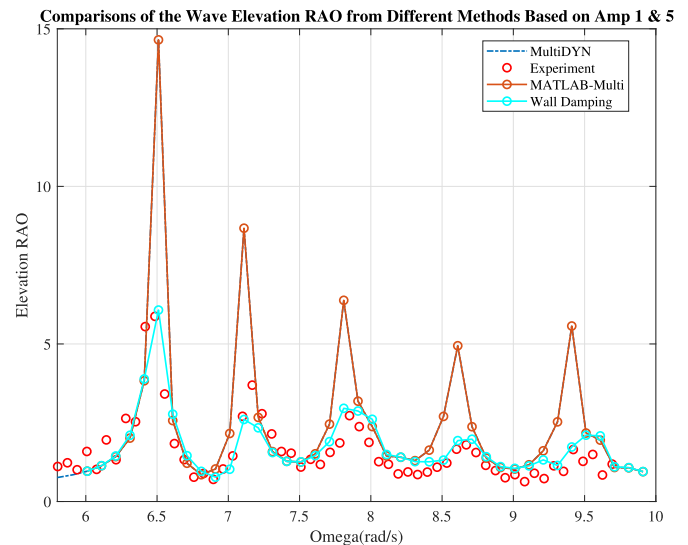
Ratio	a	b	c
Ratio of the Mean	2.4	1	3.7
Ratio of the Max Mean	3.5	1	7.6

**Fig. 10.** Damping Coefficient vs Wave Frequency.**Fig. 11.** Comparisons of results from modified potential method.

Applying the damping constants by fitting the 3 parameters, we obtain the results from the modified potential method as shown in Fig. 13. Not surprisingly, the results are almost the same with those by fitting 5 parameters.

## 5. Conclusion

We discuss the proposed method to damp out the wave elevation inside the gap. The method is a significant improvement based on the damping method applied in the sloshing problem and the coastal engineering problems. In this method, we introduce damping effect only on the ship hull. The damping effect differs by the location relative to

**Fig. 12.** Comparisons of damping constants from independent tuning and linear fitting.**Fig. 13.** Comparisons of results from modified potential method by tuning two amplitudes.

the gap. The assumption is that the damping coefficient is positively correlated with the activity level of the fluid domain. If the velocity of the fluid field is large, then the damping effect is also significant.

The method does not require the user to choose a damping domain or change the dispersion relationship. The information from the results without damping is helpful to choose the parameters of the method. We use the resonant frequencies from the linear potential method to decide the centers of the Gaussian kernel functions. The amplitudes of the Gaussian kernel functions are initially found by tuning against the experimental data. Afterwards, we find the amplitudes are approximately linear in wave frequency. Therefore, the function  $A(\omega)$  assumes a linear function in  $\omega$ . Alternatively, if we find the amplitude for the minimum and maximum resonant frequencies by tuning against the experiment, we can find the amplitudes of the Gaussian kernel function at other resonant frequencies. In this way, the shortcomings of the method is minimized.

This method is our first trial on the damping problem. If obtaining more experimental data of various floaters or different conditions in the



future, we will extend the concept of the method and improve this method using advanced techniques.

## Acknowledgments

The authors would like to thank Dr Wenhua Zhao for providing the experimental data for analysis. Also partial support was provided by Office of Naval Research under ONR Grant N000-14-16-1-2281 and Society of Naval Architects and Marine Engineers.

## References

- Teigen, P., Niedzwecki, J., 2006. A computational study of wave effects related to side-by-side LNG offloading. In: *The Sixteenth International Offshore and ...*, vol. 4. pp. 238–247.
- Buchner, B., van Dijk, a., de Wilde, J., 2001. Numerical multiple-body simulations of side-by-side mooring to an FPSO. In: *Proceedings of the Eleventh International Offshore and Polar Engineering Conference*, pp. 343–353.
- Buchner, B., Boer, G.D., Wilde, J.D., 2004. The interaction effects of mooring in close proximity of other structures. In: *The Fourteenth International Offshore and Polar Engineering Conference* ume 1. pp. 297–306.
- Bunnik, T., Pauw, W., Voogt, A., 2009. Hydrodynamic analysis for side-by-side offloading. In: *ISOPE 2009*, vol. 1. pp. 648–653.
- Chen, X., 2005. Hydrodynamic analysis for offshore LNG terminals. In: *Proc 2nd Int Workshop on Applied Offshore Hydrodynamics*.
- Chen, X.B., Malenica, S., 2005. Interaction hydrodynamique d'un ensemble de flotteurs sur la surface libre. In: *10èmes Journées de l'Hydrodynamique*, pp. 1–14 (Nantes, France).
- Faltinsen, O.M., Timokha, A.N., 2015. On damping of two-dimensional piston-mode sloshing in a rectangular moonpool under forced heave motions. *J. Fluid Mech.* 772. <https://doi.org/10.1017/jfm.2015.234>. R1.
- Faltinsen, O.M., Rognabakke, O.F., Timokha, A.N., 2007. Two-dimensional resonant piston-like sloshing in a moonpool. *J. Fluid Mech.* 575, 359. <https://doi.org/10.1017/S002211200600440X>.
- Kim, Y.-b., 2003. Dynamic Analysis of Multiple-Body Floating Platforms Coupled with Mooring Lines and Risers. Ph.D. thesis. Texas A&M University.
- Kristiansen, T., Faltinsen, O.M., 2008. Application of a vortex tracking method to the piston-like behaviour in a semi-entrained vertical gap. *Appl. Ocean Res.* 30, 1–16. <https://doi.org/10.1016/j.apor.2008.02.003>.
- Liu, Y., Falzarano, J.M., 2016a. Irregular frequency removal methods: theory and applications in hydrodynamics. *J. Mar. Sys. Ocean Technol.* 12, 49–64.
- Liu, Y., Falzarano, J.M., 2016b. Suppression of irregular frequency in multi-body problem and free-surface singularity treatment. In: *Proceedings of the ASME 2016 35th International Conference on Ocean, Offshore and Arctic Engineering*. Busan, South Korea, pp. 1–11.
- Liu, Y., Falzarano, J.M., 2017a. A method to remove irregular frequencies and log singularity evaluation in wave-body interaction problems. *J. Ocean Eng. Mar. Energy* 3, 161–189. <https://doi.org/10.1007/s40722-017-0080-z>.
- Liu, Y., Falzarano, J.M., 2017b. A note on the conclusion based on the generalized Stokes theorem. *J. Offshore Eng. Technol.* 1, 1–17.
- Liu, Y., Falzarano, J.M., 2017c. Frequency domain analysis of the interactions between multiple ships with nonzero speed in waves or current-wave interactions. In: *Proceedings of the ASME 2017 36th International Conference on Ocean, Offshore and Arctic Engineering*, Trondheim, Norway, pp. 1–17.
- Liu, Y., Falzarano, J.M., 2017d. Improvement on the accuracy of mean drift force calculation. In: *Proceedings of the ASME 2017 36th International Conference on Ocean, Offshore and Arctic Engineering*, Trondheim, Norway, pp. 1–13.
- Liu, Y., Falzarano, J.M., 2017e. Suppression of irregular frequency in multi-body problem and free-surface singularity treatment. *J. Offshore Mech. Arctic Eng.* 139, 1–16. <https://doi.org/10.1115/OMAE2016-54957>.
- Liu, Y., Falzarano, J.M., 2018. Irregular frequency effects in the calculations of the drift forces. *Ocean Sys. Eng.* 11, 1–11 (submitted).
- Liu, Y., Li, H.J., Li, Y.C., 2012. A new analytical solution for wave scattering by a submerged horizontal porous plate with finite thickness. *Ocean. Eng.* 42, 83–92. <https://doi.org/10.1016/j.oceaneng.2012.01.001>.
- Lu, L., Teng, B., Cheng, L., Sun, L., Chen, X., 2011. Modelling of multi-bodies in close proximity under water waves-Fluid resonance in narrow gaps. *Sci. China Phys. Mech. Astron.* 54, 16–25. <https://doi.org/10.1007/s11433-010-4194-8>.
- Markeng, K., 2017. Investigation of free surface damping models with applications. In: *Proceedings of the ASME 2017*, pp. 1–10.
- Miao, G., Saitoh, T., Ishida, H., 2001. Water wave interaction of twin large scale caissons with a small gap between. *Coast Eng. J.* 43, 39–58. <https://doi.org/10.1142/S0578563401000268>.
- Pauw, Willemijn, Huijsmans, Rene, Voogt, A., 2007. Advances in the hydrodynamics of side-by-side moored vessels. In: *OMAE*, vol. 2007. pp. 1–7.
- Saitoh, T., Miao, G., Ishida, H., 2006. Theoretical analysis on appearance condition of fluid resonance in a narrow gap between. In: *Proceedings of the 3rd Asia-Pacific Workshop on Marine Hydrodynamics*. China Ocean Press, Beijing, pp. 170–175.
- Sun, L., Eatock Taylor, R., Taylor, P., 2010. First- and second-order analysis of resonant waves between adjacent barges. *J. Fluid Struct.* 26, 954–978. <https://doi.org/10.1016/j.jfluidstruct.2010.06.001>.
- Wang, H., Falzarano, J.M., 2013. Energy extraction from the motion of an oscillating water column. *Ocean Sys. Eng.* 3, 327–348. <https://doi.org/10.12989/ose.2013.3.4.327>.
- Wang, H., Falzarano, J., Zhi, Y., Liu, Y., Wang, H., 2017. Energy balance analysis method in oscillating type wave converter. *J. Ocean Eng. Mar. Energy* 3, 193–208.
- Xie, Z.T., Yang, J.M., Hu, Z.Q., Zhao, W.H., Zhao, J.R., 2015. The horizontal stability of an flng with different turret locations. *Int. J. Naval Architect.* Ocean Eng. 7, 244–258. <https://doi.org/10.1515/ijnaoe-2015-0017>.
- Xie, Z., Liu, Y., Falzarano, J., 2017. A more efficient numerical evaluation of the green function in finite water depth. *Ocean Sys. Eng.* 399–412. <https://doi.org/10.12989/ose.2017.7.4.399>.
- Xie, Z., Liu, Y., Falzarano, J., 2019. A numerical evaluation of the quadratic transfer function for a floating structure. In: *Proceedings of the ASME 2019 38th International Conference on Ocean, Offshore and Arctic Engineering*, Glasgow, Scotland UK, pp. 1–14 (Submitted).
- Zalar, M., Diebold, L., Baudin, E., Henry, J., Chen, X.-b., 2007. Sloshing effects accounting for dynamic coupling between vessel and tank liquid motion. In: *OMAE 2007*, pp. 1–15.
- Zhao, W., Wolgamot, H., Draper, S., Taylor, P.H., Eatock Taylor, R., Efthymiou, M., 2016. Experimental determination of resonant response in the narrow gap between two side-by-side fixed bodies in deep water. In: *Proceedings of ASME 2016 25th International Conference on Ocean, Offshore and Arctic Engineering*, Busan, South Korea, pp. 1–7. <https://doi.org/10.1115/OMAE2016-54797>.
- Zhao, W., Lin, F., Group, R., Taylor, P.H., 2017a. Estimation of gap resonance relevant to side-by-side offloading. *Ocean. Eng.* 153, 1–10. <https://doi.org/10.1016/j.oceaneng.2018.01.056>.
- Zhao, W., Wolgamot, H.A., Taylor, P.H., Eatock Taylor, R., 2017b. Gap resonance and higher harmonics driven by focused transient wave groups. *J. Fluid Mech.* 812, 905–939. <https://doi.org/10.1017/jfm.2016.824>.
- Zhu, R., Miao, G., You, Y., 2005. Influence of gaps between 3D multiple floating structures on wave forces. *J. Hydrodyn.* 17, 141–147.
- Zhu, R., Miao, G., Zhu, H., 2006. The radiation problem of multiple structures with small gaps in between. *J. Hydrodyn, Ser. B* 18, 520–526.